

Observation of $B^\pm \rightarrow \chi_{c1}\pi^\pm$ and Search for Direct CP Violation

R. Kumar,³⁰ J. B. Singh,³⁰ K. Abe,⁶ K. Abe,⁴¹ H. Aihara,⁴³ D. Anipko,¹ T. Aushev,¹¹ T. Aziz,³⁹ A. M. Bakich,³⁸ V. Balagura,¹¹ M. Barbero,⁵ A. Bay,¹⁶ I. Bedny,¹ K. Belous,¹⁰ U. Bitenc,¹² S. Blyth,²² A. Bozek,²⁵ M. Bračko,^{6,18,12} T. E. Browder,⁵ M.-C. Chang,⁴² A. Chen,²² W. T. Chen,²² B. G. Cheon,³ R. Chistov,¹¹ Y. Choi,³⁷ S. Cole,³⁸ J. Dalseno,¹⁹ M. Dash,⁴⁷ A. Drutskoy,⁴ S. Eidelman,¹ S. Fratina,¹² N. Gabyshev,¹ T. Gershon,⁶ G. Gokhroo,³⁹ B. Golob,^{17,12} A. Gorišek,¹² H. Ha,¹⁴ J. Haba,⁶ T. Hara,²⁹ K. Hayasaka,²⁰ H. Hayashii,²¹ M. Hazumi,⁶ D. Heffernan,²⁹ T. Hokuue,²⁰ Y. Hoshi,⁴¹ S. Hou,²² W.-S. Hou,²⁴ T. Iijima,²⁰ A. Imoto,²¹ K. Inami,²⁰ R. Itoh,⁶ Y. Iwasaki,⁶ J. H. Kang,⁴⁸ N. Katayama,⁶ H. Kawai,² T. Kawasaki,²⁷ H. R. Khan,⁴⁴ H. Kichimi,⁶ K. Kinoshita,⁴ P. Krokovny,⁶ C. C. Kuo,²² Y.-J. Kwon,⁴⁸ G. Leder,⁹ S.-W. Lin,²⁴ D. Liventsev,¹¹ F. Mandl,⁹ D. Marlow,³³ T. Matsumoto,⁴⁵ A. Matyja,²⁵ W. Mitaroff,⁹ K. Miyabayashi,²¹ H. Miyake,²⁹ H. Miyata,²⁷ Y. Miyazaki,²⁰ R. Mizuk,¹¹ G. R. Moloney,¹⁹ J. Mueller,³² E. Nakano,²⁸ M. Nakao,⁶ S. Nishida,⁶ O. Nitoh,⁴⁶ S. Noguchi,²¹ T. Ohshima,²⁰ T. Okabe,²⁰ S. Okuno,¹³ S. L. Olsen,⁵ Y. Onuki,²⁷ H. Ozaki,⁶ P. Pakhlov,¹¹ G. Pakhlova,¹¹ H. Palka,²⁵ H. Park,¹⁵ K. S. Park,³⁷ R. Pestotnik,¹² L. E. Piilonen,⁴⁷ Y. Sakai,⁶ T. Schietinger,¹⁶ O. Schneider,¹⁶ J. Schümamm,²³ C. Schwanda,⁹ A. J. Schwartz,⁴ R. Seidl,^{7,34} M. Shapkin,¹⁰ H. Shibuya,⁴⁰ B. Shwartz,¹ V. Sidorov,¹ A. Sokolov,¹⁰ A. Somov,⁴ N. Soni,³⁰ M. Starič,¹² H. Stoeck,³⁸ S. Suzuki,³⁵ F. Takasaki,⁶ M. Tanaka,⁶ G. N. Taylor,¹⁹ Y. Teramoto,²⁸ X. C. Tian,³¹ I. Tikhomirov,¹¹ K. Trabelsi,⁵ T. Tsuboyama,⁶ T. Tsukamoto,⁶ S. Uehara,⁶ T. Uglov,¹¹ K. Ueno,²⁴ S. Uno,⁶ Y. Usov,¹ G. Varner,⁵ S. Villa,¹⁶ C. C. Wang,²⁴ C. H. Wang,²³ M.-Z. Wang,²⁴ Y. Watanabe,⁴⁴ E. Won,¹⁴ Q. L. Xie,⁸ A. Yamaguchi,⁴² Y. Yamashita,²⁶ M. Yamauchi,⁶ C. C. Zhang,⁸ L. M. Zhang,³⁶ Z. P. Zhang,³⁶ and A. Zupanc¹²

(The Belle Collaboration)

¹*Budker Institute of Nuclear Physics, Novosibirsk*

²*Chiba University, Chiba*

³*Chonnam National University, Kwangju*

⁴*University of Cincinnati, Cincinnati, Ohio 45221*

⁵*University of Hawaii, Honolulu, Hawaii 96822*

⁶*High Energy Accelerator Research Organization (KEK), Tsukuba*

⁷*University of Illinois at Urbana-Champaign, Urbana, Illinois 61801*

⁸*Institute of High Energy Physics, Chinese Academy of Sciences, Beijing*

⁹*Institute of High Energy Physics, Vienna*

¹⁰*Institute of High Energy Physics, Protvino*

¹¹*Institute for Theoretical and Experimental Physics, Moscow*

¹²*J. Stefan Institute, Ljubljana*

¹³*Kanagawa University, Yokohama*

¹⁴*Korea University, Seoul*

¹⁵*Kyungpook National University, Taegu*

¹⁶*Swiss Federal Institute of Technology of Lausanne, EPFL, Lausanne*

¹⁷*University of Ljubljana, Ljubljana*

¹⁸*University of Maribor, Maribor*

¹⁹*University of Melbourne, Victoria*

²⁰*Nagoya University, Nagoya*

²¹*Nara Women's University, Nara*

²²*National Central University, Chung-li*

²³*National United University, Miao Li*

²⁴*Department of Physics, National Taiwan University, Taipei*

²⁵*H. Niewodniczanski Institute of Nuclear Physics, Krakow*

²⁶*Nippon Dental University, Niigata*

²⁷*Niigata University, Niigata*

²⁸*Osaka City University, Osaka*

²⁹*Osaka University, Osaka*

³⁰*Panjab University, Chandigarh*

³¹*Peking University, Beijing*

³²*University of Pittsburgh, Pittsburgh, Pennsylvania 15260*

³³*Princeton University, Princeton, New Jersey 08544*

³⁴*RIKEN BNL Research Center, Upton, New York 11973*

³⁵*Saga University, Saga*

³⁶*University of Science and Technology of China, Hefei*

³⁷*Sungkyunkwan University, Suwon*

³⁸*University of Sydney, Sydney NSW*

³⁹Tata Institute of Fundamental Research, Bombay

⁴⁰Toho University, Funabashi

⁴¹Tohoku Gakuin University, Tagajo

⁴²Tohoku University, Sendai

⁴³Department of Physics, University of Tokyo, Tokyo

⁴⁴Tokyo Institute of Technology, Tokyo

⁴⁵Tokyo Metropolitan University, Tokyo

⁴⁶Tokyo University of Agriculture and Technology, Tokyo

⁴⁷Virginia Polytechnic Institute and State University, Blacksburg, Virginia 24061

⁴⁸Yonsei University, Seoul

We report the first observation of $B^\pm \rightarrow \chi_{c1}\pi^\pm$, a Cabibbo- and color-suppressed decay in a data sample of 386×10^6 $B\bar{B}$ events collected at the $\Upsilon(4S)$ resonance with the Belle detector at the KEKB asymmetric-energy e^+e^- collider. We observe 55 ± 10 signal events with a statistical significance of 6.3σ including systematic uncertainties. The measured branching fraction and charge-asymmetry is $\mathcal{B}(B^\pm \rightarrow \chi_{c1}\pi^\pm) = (2.2 \pm 0.4 \pm 0.3) \times 10^{-5}$ and $\mathcal{A}_\pi = 0.07 \pm 0.18 \pm 0.02$, respectively. We also determine the ratio $\mathcal{B}(B^\pm \rightarrow \chi_{c1}\pi^\pm)/\mathcal{B}(B^\pm \rightarrow \chi_{c1}K^\pm) = (4.3 \pm 0.8 \pm 0.3)\%$.

PACS numbers: 13.25.Hw, 14.40.Gx, 14.40.Nd

Decays of B -mesons to two-body final states including charmonium are expected to occur predominantly via the color-suppressed spectator diagram as shown in Fig. 1. The branching fraction for the $B^- \rightarrow \chi_{c1}K^-$ [1] decay mode is well measured by Belle and BaBar [2, 3]. To produce this final state, the vector current (W^-) couples to a $\bar{c}s$ pair; the s -quark and spectator anti-quark hadronize into a kaon. If this theoretical description is correct, a corresponding Cabibbo-suppressed decay mode should exist, where the vector current couples to a $\bar{c}d$ pair. The d -quark and spectator anti-quark hadronize as a pion, which leads to a $B^- \rightarrow \chi_{c1}\pi^-$ decay. If the leading-order tree level diagram is the dominant contribution, the factorization picture implies that the branching fraction of $B^- \rightarrow \chi_{c1}\pi^-$ decay mode should be $\sim 5\%$ of that of the Cabibbo-allowed $B^- \rightarrow \chi_{c1}K^-$ decay mode [4]. The Standard Model predicts that for $b \rightarrow c\bar{c}s$ decays, the tree and penguin contributions have a small relative weak phase. Therefore, negligible direct CP -violation is expected in $B^\pm \rightarrow \chi_{c1}K^\pm$ decay. In $b \rightarrow c\bar{c}d$ transitions, however, tree and penguin contributions have different phases and direct CP -violation may be as large as a few percent [5, 6].

In this paper, we report the first observation of $B^- \rightarrow \chi_{c1}\pi^-$ decay. A measurement of the ratio of branching fractions $\mathcal{B}(B^- \rightarrow \chi_{c1}\pi^-)/\mathcal{B}(B^- \rightarrow \chi_{c1}K^-)$ and a search for direct CP -violation in $B^\pm \rightarrow \chi_{c1}\pi^\pm$ decays is also presented. We use a data sample containing $(386 \pm 5) \times 10^6$ $B\bar{B}$ events collected at the $\Upsilon(4S)$ resonance with the Belle detector [7] at the KEKB asymmetric-energy e^+e^- collider [8].

The Belle detector is a large solid-angle magnetic spectrometer located at the KEKB e^+e^- storage rings, which collide 8.0 GeV electrons with 3.5 GeV positrons producing a center-of-mass (CM) energy of 10.58 GeV, the mass of the $\Upsilon(4S)$ resonance. Closest to the interaction point (IP) is a silicon vertex detector (SVD), surrounded by a 50-layer central drift chamber (CDC), an array of aerogel Cherenkov counters (ACC), a barrel-like ar-

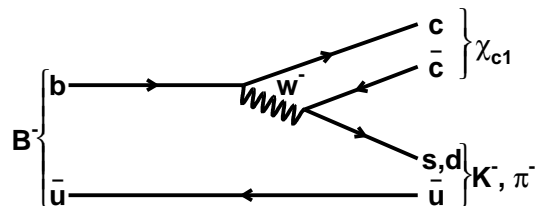


FIG. 1: Leading-order tree level diagram for the decays under study.

range of time-of-flight (TOF) scintillation counters, and an electromagnetic calorimeter (ECL) comprised of CsI(Tl) crystals. These subdetectors are located inside a superconducting solenoid coil that provides a 1.5 T magnetic field. An iron flux-return yoke located outside the coil is instrumented to detect K_L^0 mesons and to identify muons. The detector is described in detail elsewhere [7]. The data set consists of two subsets: the first 152×10^6 B -meson pairs were collected with a 2.0 cm radius beam-pipe and a 3-layer SVD, and the remaining 234×10^6 B -meson pairs with a 1.5 cm radius beam-pipe, a 4-layer SVD and a small-cell inner drift chamber [9].

Events with B -meson candidates are first selected by applying general hadronic event selection criteria. These include a requirement on charged tracks (at least three of them should originate from an event vertex consistent with the IP), a requirement on the reconstructed CM energy ($E^{CM} > 0.2\sqrt{s}$, where \sqrt{s} is the total CM energy), a requirement on the longitudinal (z -direction) component of the reconstructed CM momentum with respect to the beam direction ($|p_z^{CM}| < 0.5\sqrt{s}/c$), and a requirement on the total ECL energy ($0.1\sqrt{s} < E_{ECL}^{CM} < 0.8\sqrt{s}$) with at least two energy clusters. To suppress continuum background, we reject events where the ratio of the second to zeroth Fox-Wolfram moments [10] is greater than 0.5. To remove charged particle tracks that are poorly measured

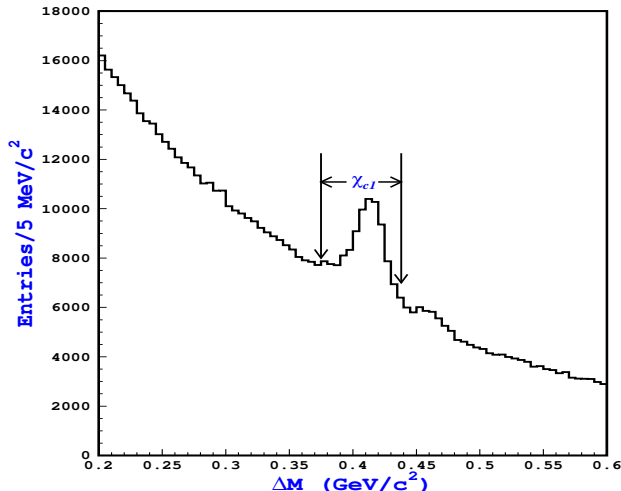


FIG. 2: The ΔM ($M_{\ell^+\ell^-\gamma} - M_{\ell^+\ell^-}$) distribution for the χ_{c1} candidates. The arrows indicate the selected mass region. The enhancement just above the χ_{c1} mass region is due to the χ_{c2} .

or do not come from the interaction region, we require their origin to be within 0.5 cm of the IP in the radial direction, and 5 cm along the beam direction (z -direction).

We reconstruct the χ_{c1} state via the decay mode $\chi_{c1} \rightarrow \gamma J/\psi$. We begin by reconstructing $J/\psi \rightarrow \ell^+\ell^-$ candidates, where ℓ is a muon or electron. For muon tracks, identification is based on track penetration depth and the hit pattern in the KLM system. Electron tracks are identified by a combination of dE/dx from the CDC, E/p (E is the energy deposited in the ECL and p is the momentum measured by the SVD and the CDC), and shower shape in the ECL. In order to recover dielectron events in which one or both electrons radiate a photon, the four-momenta of all photons within 0.05 radians of the e^+ or e^- directions are included in the invariant mass calculation. The invariant mass window used to select J/ψ candidates in the $\mu^+\mu^-(e^+e^-)$ channel is -0.06 (-0.15) $\text{GeV}/c^2 \leq M_{\ell^+\ell^-} - m_{J/\psi} \leq 0.036$ GeV/c^2 , where $m_{J/\psi}$ denotes the nominal J/ψ mass [11]; these intervals are asymmetric in order to include part of the radiative tails. Vertex- and mass-constrained kinematic fits are performed for selected J/ψ candidates to improve the momentum resolution.

Photons are identified as ECL energy clusters that are not associated with a charged track and have a minimum energy of 0.060 GeV. We reject the photon candidate if the ratio of the energy in the array of the central 3×3 ECL cells to that in the array of 5×5 cells is less than 0.87.

To reconstruct the χ_{c1} state, we combine a J/ψ candidate with momentum below 2.0 GeV/c in the CM frame with a selected photon. To suppress photons arising from $\pi^0 \rightarrow \gamma\gamma$, we veto photons that, when combined with an-

other photon in the event, satisfy $0.110 \text{ GeV}/c^2 \leq M_{\gamma\gamma} \leq 0.150 \text{ GeV}/c^2$. The χ_{c1} candidates are selected by requiring the mass difference ($\Delta M = M_{\ell^+\ell^-\gamma} - M_{\ell^+\ell^-}$) to lie between 0.370 GeV/c^2 and 0.438 GeV/c^2 . The ΔM distribution is shown in Fig. 2. A mass-constrained fit is applied to all selected χ_{c1} candidates in order to improve the momentum resolution.

Charged pions and kaons are identified using energy loss measurements in the CDC, Cherenkov light yields in the ACC, and TOF information. The information from these detectors is combined to form π - K likelihood ratio, $\mathcal{R}(\pi/K) = \mathcal{L}_\pi / (\mathcal{L}_\pi + \mathcal{L}_K)$, where \mathcal{L}_π (\mathcal{L}_K) is the likelihood that a pion (kaon) would produce the observed detector response. Charged tracks with $\mathcal{R}(\pi/K) > 0.9$ are selected as charged pions, and tracks with $\mathcal{R}(\pi/K) \leq 0.4$ are selected as charged kaons. The efficiency for pion (kaon) identification is 75.1% (86.1%) and the probability of kaon (pion) misidentification is 4.6% (10.5%) with the above criteria. We determine the selection criteria by optimizing the figure of merit, $S/\sqrt{(S+B)}$, where S (B) is the number of signal (background) events in the signal region, with an assumed branching fraction that is 5% of that for $B^- \rightarrow \chi_{c1}K^-$ [11].

We reconstruct B -mesons by combining a χ_{c1} candidate with a charged pion or kaon. The energy difference, $\Delta E \equiv E_B^* - E_{\text{beam}}^*$ and the beam-constrained mass $M_{\text{bc}} \equiv \sqrt{E_{\text{beam}}^{*2} - p_B^{*2}}$, are used to separate signal from background, where E_{beam}^* is the run dependent beam energy, and E_B^* and p_B^* are the reconstructed energy and momentum, respectively, of the B -meson candidates in the CM frame. We accept candidates in the region $5.27 \text{ GeV}/c^2 \leq M_{\text{bc}} \leq 5.29 \text{ GeV}/c^2$ and $|\Delta E| < 0.2$ (0.15) GeV for the $B^- \rightarrow \chi_{c1}\pi^-$ (K^-) mode. When an event contains more than one B -meson candidate passing the above requirements (this occurs in $\sim 2.5\%$ of the candidate events), the candidate with M_{bc} closest to the nominal B^- mass [11] is selected.

We extract the signal yields by performing a binned maximum likelihood fit to the ΔE distribution of the selected candidates. For the $B^- \rightarrow \chi_{c1}K^-$ mode, we fit with a sum of two Gaussians for signal and a second-order polynomial for background. In the fit for the $B^- \rightarrow \chi_{c1}\pi^-$ mode, a background component exists due to misidentified $\chi_{c1}K^-$. This background has a peak at $\Delta E \sim -0.07$ GeV and is modeled by a sum of two bifurcated Gaussians. A third-order polynomial is used for the sum of all other backgrounds. We study backgrounds using a large sample of inclusive charmonium Monte Carlo (MC) events [12]. Except for the misidentified $B^- \rightarrow \chi_{c1}K^-$ background, no structure is observed in the ΔE distribution. However, the M_{bc} distribution has a peaking component. Therefore, we use the ΔE distributions for the signal extraction. The scatter plot of ΔE versus M_{bc} for $B^- \rightarrow \chi_{c1}\pi^-$ candidates is shown in Fig. 3, where the M_{bc} requirement is loosened to 5.2 GeV/c^2 .

All parameters of the fitting functions are floated in the fit of the $B^- \rightarrow \chi_{c1}K^-$ mode. For the $B^- \rightarrow \chi_{c1}\pi^-$

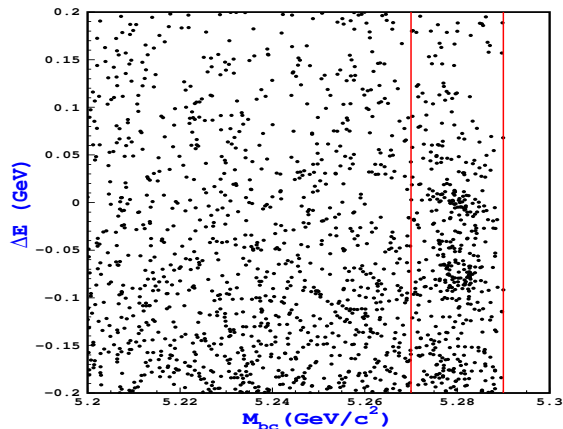


FIG. 3: The scatter plot of ΔE versus M_{bc} for $B^\pm \rightarrow \chi_{c1}\pi^\pm$ candidates, where the two vertical lines indicate the M_{bc} region used for signal extraction.

mode, the signal shape is fixed to that obtained from the $B^- \rightarrow \chi_{c1}K^-$ mode. The shape of misidentified $\chi_{c1}K^-$ background is initially determined from a MC sample, with a correction applied to account for the small difference between data and MC in the $B^- \rightarrow \chi_{c1}K^-$ sample. We obtain 1597 ± 48 and 55 ± 10 signal events for $B^- \rightarrow \chi_{c1}K^-$ and $B^- \rightarrow \chi_{c1}\pi^-$ modes, respectively. The ΔE distributions are shown in Figs. 4 and 5, together with the fit results. The number of misidentified $B^- \rightarrow \chi_{c1}K^-$ events obtained from the fit to Fig. 5 is 61 ± 14 . This is consistent with the expectation from the observed $B^- \rightarrow \chi_{c1}K^-$ signal yield (Fig. 4) given the probability of misidentifying a kaon as a pion. The significance of the $B^- \rightarrow \chi_{c1}\pi^-$ signal is 6.3σ , where the significance is defined as $\sqrt{-2\ln(\mathcal{L}_0/\mathcal{L}_{\max})}$ and \mathcal{L}_{\max} (\mathcal{L}_0) denotes the likelihood value at the maximum (with the signal yield fixed at zero). We include the effect of systematic error in this calculation by subtracting a quadratic sum of the variations of the significance in smaller direction when each fixed parameter in the fit is changed by $\pm 1\sigma$.

The branching fraction for the $B^- \rightarrow \chi_{c1}\pi^-$ decay mode is calculated by dividing the observed signal yield by the reconstruction efficiency, the number of $B\bar{B}$ events in the data sample, and the daughter branching fractions. We determine the reconstruction efficiency (17.3%) from signal MC events, where the correction for difference between data and MC has been applied for the pion identification requirement (0.90 ± 0.01) and the ΔM requirement (0.97 ± 0.03). The correction factor for the ΔM requirement is determined from the $B^- \rightarrow \chi_{c1}K^-$ sample and is estimated by taking the ratio of yields from data and MC for tight ($0.370 \text{ GeV}/c^2 < \Delta M < 0.438 \text{ GeV}/c^2$) and loose ($0.3 \text{ GeV}/c^2 < \Delta M < 0.5 \text{ GeV}/c^2$) ΔM windows. We use the daughter branching fractions published in Particle Data Book 2004 [11]. Equal production of neutral and charged B -meson pairs in $\Upsilon(4S)$ decay is as-

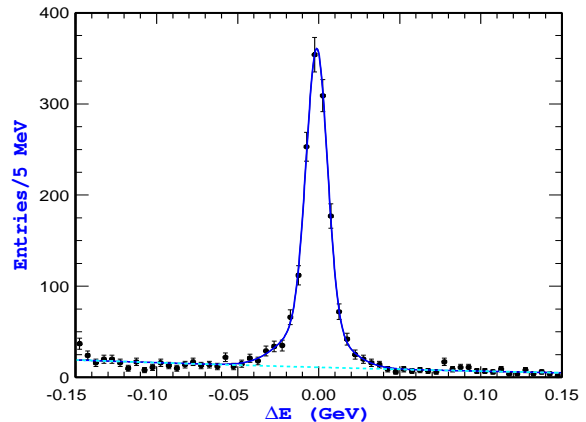


FIG. 4: The ΔE distribution for the $B^\pm \rightarrow \chi_{c1}K^\pm$ decay mode. The solid and dashed curves show the total fit and the polynomial background component of the fit, respectively.

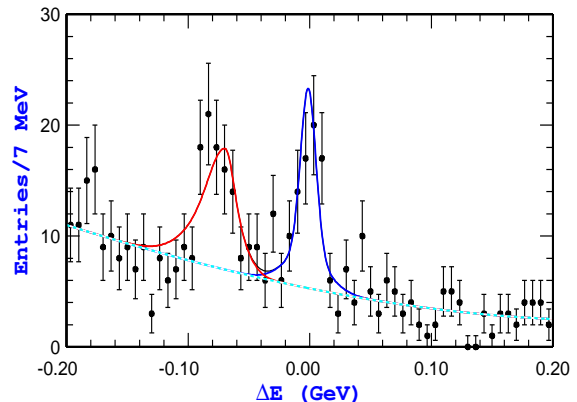


FIG. 5: The ΔE distribution for the $B^\pm \rightarrow \chi_{c1}\pi^\pm$ decay mode. The signal peak is seen around zero. The peak at -0.07 GeV is from $B^\pm \rightarrow \chi_{c1}K^\pm$ decay. The solid and dashed curves show the total fit and the polynomial background component of the fit, respectively.

sumed. The resulting branching fraction is

$$\mathcal{B}(B^\pm \rightarrow \chi_{c1}\pi^\pm) = (2.2 \pm 0.4 \pm 0.3) \times 10^{-5}, \quad (1)$$

where the first error is statistical and the second is systematic. We obtain the branching fraction for the $B^- \rightarrow \chi_{c1}K^-$ decay mode by similar procedures. The result, $(51.4 \pm 1.5) \times 10^{-5}$, (error is statistical only) is consistent with the previous measurements [2, 3]. The ratio of branching fractions is

$$\frac{\mathcal{B}(B^- \rightarrow \chi_{c1}\pi^-)}{\mathcal{B}(B^- \rightarrow \chi_{c1}K^-)} = (4.3 \pm 0.8 \pm 0.3)\%, \quad (2)$$

which is consistent with expectations from the factorization model [4].

The systematic uncertainties are summarized in Table I. Since the shape used for the signal is fixed in the

TABLE I: Summary of systematic errors on branching fraction.

Source	Uncertainty (%)
Uncertainty in yield	5.9
Tracking error	3.0
Lepton Identification	4.0
PID (pion)	1.0
γ detection	2.0
ΔM requirement	3.0
MC statistics	0.9
$N_{B\bar{B}}$	1.2
Daughter branching fractions	10.6
Total	13.7

fit to Fig. 5, we repeat the fit, varying each fixed shape parameter by the $\pm 1\sigma$ uncertainty in our determination of it from external samples (Fig. 4 and MC). The systematic uncertainty on the signal yield is then calculated by taking the quadratic sum of the deviations in the signal yield from the nominal value. We checked for possible bias in the fitting using a MC sample; no significant bias was found. The systematic uncertainty assigned to the yield is 5.9%. The uncertainty on the tracking efficiency is estimated to be 1.0% per track, while that due to lepton identification is 2.0% per lepton, and 1.0% (1.3%) per pion (kaon) identification (PID). We assign an uncertainty of 2.0% for the γ detection efficiency. The systematic uncertainty due to $\chi_{c1} \rightarrow \gamma J/\psi$ and $J/\psi \rightarrow \ell^+ \ell^-$ branching fractions is 10.6%. The total systematic error is the sum of all the above uncertainties in quadrature.

Many of the systematic errors cancel for the ratio of branching fractions; contributions come from only the uncertainty in the $B^- \rightarrow \chi_{c1} \pi^-$ yield, PID (1.0% for $B^- \rightarrow \chi_{c1} K^-$), and MC statistics (1.0% for $B^- \rightarrow \chi_{c1} K^-$).

The CP -violating charge asymmetry \mathcal{A}_i is defined as

$$\mathcal{A}_i = \frac{N_i^- - N_i^+}{N_i^- + N_i^+}; \quad i = \pi, K. \quad (3)$$

Here, N_i^- and N_i^+ are the signal yields for negative and positive B -meson decays and are measured separately by using the method described above. For the $B^- \rightarrow \chi_{c1} \pi^-$ mode, the polynomial background shape is fixed to that obtained for the branching fraction measurement.

The measured charge asymmetries for the $B^\pm \rightarrow \chi_{c1} \pi^\pm (K^\pm)$ decay modes are listed in Table II. No significant asymmetries are seen in either decay modes. The systematic errors on \mathcal{A}_π (\mathcal{A}_K) include: uncertainty in

yield extraction, 0.007; possible difference between B^- and B^+ signal shape parameters, 0.002 (0.001); possible charge asymmetry in pion (kaon) identification efficiency 0.014 (0.011); and possible detector bias 0.016, which is estimated from the charge asymmetry of the $B^\pm \rightarrow J/\psi K^\pm$ decay sample without a PID requirement.

TABLE II: Summary of charge asymmetries. First (second) error is statistical (systematic).

Mode	Yield(-)	Yield(+)	\mathcal{A}
$B^\pm \rightarrow \chi_{c1} \pi^\pm$	29 ± 7	25 ± 7	$0.07 \pm 0.18 \pm 0.02$
$B^\pm \rightarrow \chi_{c1} K^\pm$	792 ± 31	807 ± 31	$-0.01 \pm 0.03 \pm 0.02$

In summary, we report the first observation of $B^- \rightarrow \chi_{c1} \pi^-$ decay with $386 \times 10^6 B\bar{B}$ events. The observed signal yield is 55 ± 10 with a significance of 6.3σ including systematic uncertainty. The measured branching fraction is $\mathcal{B}(B^\pm \rightarrow \chi_{c1} \pi^\pm) = (2.2 \pm 0.4 \pm 0.3) \times 10^{-5}$. The ratio $\mathcal{B}(B^- \rightarrow \chi_{c1} \pi^-)/\mathcal{B}(B^- \rightarrow \chi_{c1} K^-) = (4.3 \pm 0.8 \pm 0.3)\%$, which is consistent with the Standard Model prediction. While the accuracy of \mathcal{A}_K is improved from the previous measurement [3], no significant CP -violating charge asymmetries are observed in either $B^\pm \rightarrow \chi_{c1} \pi^\pm$ or $B^\pm \rightarrow \chi_{c1} K^\pm$ decay modes.

We thank the KEKB group for the excellent operation of the accelerator, the KEK cryogenics group for the efficient operation of the solenoid, and the KEK computer group and the National Institute of Informatics for valuable computing and Super-SINET network support. We acknowledge support from the Ministry of Education, Culture, Sports, Science, and Technology of Japan and the Japan Society for the Promotion of Science; the Australian Research Council and the Australian Department of Education, Science and Training; the National Science Foundation of China and the Knowledge Innovation Program of the Chinese Academy of Sciences under contract No. 10575109 and IHEP-U-503; the Department of Science and Technology of India; the BK21 program of the Ministry of Education of Korea, the CHEP SRC program and Basic Research program (grant No. R01-2005-000-10089-0) of the Korea Science and Engineering Foundation, and the Pure Basic Research Group program of the Korea Research Foundation; the Polish State Committee for Scientific Research; the Ministry of Science and Technology of the Russian Federation; the Slovenian Research Agency; the Swiss National Science Foundation; the National Science Council and the Ministry of Education of Taiwan; and the U.S. Department of Energy.

[1] Charge-conjugate modes are included throughout this paper unless stated otherwise.

[2] N. Soni *et al.* (Belle Collaboration), Phys. Lett. B **634**,

155 (2006).

[3] B. Aubert *et al.* (BaBar Collaboration), Phys. Rev. Lett. **94**, 141801 (2005).

- [4] M. Neubert and B. Stech, in *Heavy flavours II*, eds. A.J. Buras and M. Linder (World Scientific, Singapore, 1988) pp. 345.
- [5] M. Gronau, Phys. Rev. Lett. **63**, 1451 (1989).
- [6] I. Dunietz, Phys. Lett. B **316**, 561 (1993).
- [7] A. Abashian *et al.* (Belle Collaboration), Nucl. Instrum. and Meth. A **479**, 117 (2002).
- [8] S. Kurokawa and E. Kikutani, Nucl. Instrum. and Meth. A **499**, 1 (2003).
- [9] Y. Ushiroda, Nucl. Instrum. and Meth. A **511**, 6 (2003).
- [10] G. Fox and S. Wolfram, Phys. Rev. Lett. **41**, 1581 (1978).
- [11] S. Eidelman *et al.* (Particle Data Group), Phys. Lett. B **592**, 1 (2004).
- [12] We use the EvtGen *B*-meson decay generator developed by the CLEO and BaBar Collaborations, see: <http://www.slac.stanford.edu/~lange/EvtGen/>. The detector response is simulated by a program based on GEANT-3, CERN program library long writeup W5013, CERN, (1993).